Constraining dark-matter ensembles with supernova data

Aditi Desai, ^{1,*} Keith R. Dienes, ^{2,3,†} and Brooks Thomas, ^{1,‡} ¹Department of Physics, Lafayette College, Easton, Pennsylvania 18042 USA, ²Department of Physics, University of Arizona, Tucson, Arizona 85721 USA, ³Department of Physics, University of Maryland, College Park, Maryland 20742 USA

(Received 6 October 2019; accepted 23 January 2020; published 24 February 2020)

The constraints on nonminimal dark sectors involving ensembles of unstable dark-matter species are well established and quite stringent in cases in which these species decay to visible-sector particles. However, in cases in which these ensembles decay exclusively to other, lighter dark-sector states, the corresponding constraints are less well established. In this paper, we investigate how information about the expansion rate of the universe at low redshifts gleaned from observations of Type Ia supernovae can be used to constrain ensembles of unstable particles which decay primarily into dark radiation.

DOI: 10.1103/PhysRevD.101.035031

I. INTRODUCTION

Dynamical Dark Matter (DDM) [1,2] is an alternative framework for dark-matter physics in which the dark matter is an ensemble comprising a potentially vast number of different constituent particle species whose properties (masses, lifetimes, cosmological abundances, etc.) scale across the ensemble according to a set of scaling relations. The specific scaling relations depend on the underlying physics of the particular DDM model in question. In all cases, however, these scaling relations lead to a balancing of decay widths against cosmological abundances across the ensemble such that the abundances of the more unstable constituents are suppressed. In this way, the DDM framework circumvents the stringent bounds on dark-matter decays in traditional dark-matter scenarios—scenarios in which the dark-matter candidate χ has a single, welldefined lifetime τ_{γ} .

Observational constraints on dark-matter decay—together with the traditional assumption that χ contributes essentially the entirety of the total present-day dark-matter abundance—impose a stringent lower bound on τ_{χ} . Indeed, in such scenarios, one finds that χ must be "hyperstable," with a lifetime which significantly exceeds the present age of the universe. By contrast, within the DDM framework, a nontrivial fraction of the total abundance of the dark-matter ensemble can be carried by particle species with lifetimes well below the timescale associated with this hyperstability bound without violating the same observational constraints. In this way, the DDM framework evades the stringent bounds that arise for dark-matter decays in traditional

dark-matter scenarios, thereby broadening the theory space of viable decaying-dark-matter models. Moreover, realizations of this framework can give rise to novel signatures at colliders [3,4], at dedicated long-lived-particle detectors [5,6], at direct-detection experiments [7], and at indirect-detection experiments [8–10].

The hyperstability bound on the lifetime of a traditional dark-matter candidate depends crucially on the final states into which it decays. In scenarios in which χ decays with a non-negligible branching fraction into final states involving any Standard-Model (SM) particles other than neutrinos, constraints on the diffuse photon flux from Fermi-LAT [11] imply a hyperstability bound of $\tau_{\gamma} \gtrsim \mathcal{O}(10^{28} \text{ s})$ for darkmatter masses in the range $\mathcal{O}(100 \text{ MeV}) \lesssim m_{\gamma} \lesssim \mathcal{O}(\text{EeV})$ [12–15]. The corresponding constraints for a dark-matter mass in the range $\mathcal{O}(10 \text{ keV}) \lesssim m_{\gamma} \lesssim \mathcal{O}(100 \text{ MeV})$ from measurements of the diffuse photon flux at lower energies [16] and from CMB data [17], while slightly more dependent on the channels through which γ decays, are nevertheless quite stringent. Measurements of the positron flux by the AMS-02 detector [18,19] also imply constraints of roughly the same order on dark-matter decays to a wide variety of final states [20].

By contrast, if the dark-matter candidate decays exclusively to other, lighter states within the dark sector, the hyperstability bound on its lifetime is far weaker. The leading constraints on dark-matter decays of this sort ultimately stem from the fact that the conversion of the mass energy of the decaying dark-matter particles into the kinetic energy of their decay products alters the effective equation of state of the dark sector as a whole. This in turn leads a modification of the expansion history of the universe relative to the prediction of the standard cosmology. Such a modification would not only leave imprints both in the power spectrum of the CMB and in the matter

^{*}desaia@lafayette.edu

dienes@email.arizona.edu

[‡]thomasbd@lafayette.edu

power spectrum, but would also be evident in baryon acoustic oscillations (BAO) and in Type Ia supernova data, both of which provide an observational handle on the expansion history at low redshifts. Taken together, these considerations place the hyperstability bound on the lifetime of a traditional dark-matter candidate which decays exclusively to other states within the dark sector at around $\tau_{\chi} \gtrsim 2 \times 10^{19} \ \mathrm{s} \ [21,22]$.

Within explicit realizations of the DDM framework, such as those described in Refs. [23–25], the situation can be different. Indeed, much effort has already been devoted to determining the extent to which the hyperstability bound on dark-matter decays into visible-sector particles can be circumvented in such cases. However, the extent to which the hyperstability bound on dark-matter decays solely to other particles within the dark sector can be circumvented within this framework has yet to be explored. In this paper, we take a first step in this direction. In particular, we investigate how information about the expansion rate of the universe at low redshifts gleaned from the relationship between the redshifts and luminosity distances of Type Ia supernovae can be used to constrain DDM ensembles which decay primarily to other, lighter states within the dark sector which act as dark radiation. This technique for constraining decays within the dark sector, which has previously been applied to scenarios involving a single unstable particle species [26,27], is particularly relevant for constraining scenarios within the DDM framework.

The outline of this paper is as follows. In Sec. II, we describe the DDM model on which we shall focus in this paper. As we shall see, this model is representative of a large class of models within the DDM framework. In Sec. III, we derive an expression for the luminosity distance $d_L(z)$ as a function of cosmological redshift z for an ensemble of unstable particles which decay to other, lighter states within the dark sector. In Sec. IV, we describe the catalog of Type Ia supernovae we use in order to constrain the relationship between redshift and luminosity distance in scenarios involving dark-to-dark decays. We also outline our statistical method for assessing the goodness of fit between the functional form of $d_L(z)$ obtained within any such scenario and the set of measured redshifts and luminosity distances for the supernovae within this data set. Finally, in Sec. V, we present our results and assess the extent to which our DDM parameter space can be constrained by supernova data. In Sec. VI, we conclude with a summary of our findings and a discussion of possible avenues for future work.

II. PARAMETRIZING THE DDM ENSEMBLE

Within the DDM framework, the dark-matter candidate is an ensemble comprising a large number N of individual constituent particle species χ_n , where the index n = 0, 1, 2, ..., N - 1 labels the particles in order of increasing

mass. In many realizations of DDM, the spectrum of masses m_n for these ensemble constituents takes the form

$$m_n = m_0 + n^\delta \Delta m, \tag{2.1}$$

where m_0 denotes the mass of the lightest ensemble constituent, where Δm is a free parameter with dimensions of mass, and where δ is a dimensionless scaling exponent.

For simplicity, we shall assume that each ensemble constituent decays with a branching fraction of essentially unity via the process $\chi_n \to \bar{\psi}\psi$, where ψ is a massless dark-sector particle which behaves as dark radiation. Moreover, we shall also assume that the total decay widths Γ_n of the χ_n scale across the ensemble according to a power law of the form

$$\Gamma_n = \Gamma_0 \left(\frac{m_n}{m_0}\right)^{\xi},\tag{2.2}$$

where Γ_0 denotes the decay width of the lightest particle in the ensemble and where ξ is another dimensionless scaling exponent. In what follows, we take Γ_0 and ξ to be free parameters.

We note that intra-ensemble decays—i.e., decays of the ensemble constituents into final states which include other, lighter χ_n —represent another important class of dark-todark decays which can potentially occur within the DDM framework. Indeed, such decays arise in many realizations of the DDM framework. While we shall not consider intraensemble decays in this analysis, we note that supernova constraints on scenarios in which one or more of the ensemble constituents have non-negligible branching fractions into final states involving other, lighter χ_n are generically weaker than the bounds on scenarios in which the ensemble constituents decay to states involving dark radiation alone. This is because these constraints ultimately follow from deviations in the expansion rate of the universe as a function of redshift from the expected relationship obtained within a Λ_{CDM} cosmology. Thus, the constraints we shall derive in this paper for a given DDM model represent a conservative bound on extensions of this same model involving intra-ensemble decays.

We shall assume that the initial abundances Ω_n for the individual ensemble constituents are established at some early time $t_{\rm prod}$. We shall assume that $t_{\rm prod} \ll t_{\rm LS} \approx 1.17 \times 10^{13} \, {\rm s}$, where $t_{\rm LS}$ denotes the time of last scattering, and that $t_{\rm prod} \ll \tau_{N-1}$. However, provided that these two criteria are satisfied, our results in what follows will be independent of $t_{\rm prod}$. In order to retain as much generality as possible, we shall remain largely agnostic about the mechanism which generates these abundances. However, we shall assume that the cosmological population of each ensemble constituent can be considered to be "cold," in the sense that its equation-of-state parameter may be taken to be $w_n \approx 0$ for all $t > t_{\rm prod}$. Moreover, for concreteness, we shall assume that the initial

abundances $\Omega_n(t_{\mathrm{prod}})$ of the individual ensemble constituents at $t=t_{\mathrm{prod}}$ scale across the ensemble according to a power law of the form

$$\Omega_n(t_{\text{prod}}) = \Omega_0(t_{\text{prod}}) \left(\frac{m_n}{m_0}\right)^{\gamma},$$
(2.3)

where $\Omega_0(t_{\mathrm{prod}})$ denotes the initial abundance of the lightest ensemble constituent and where γ is a dimensionless scaling exponent. We take this scaling exponent to be a free parameter. By contrast, as we shall discuss in further detail in Sec. IV, the value of $\Omega_0(t_{\mathrm{prod}})$ is essentially fixed by the requirement that the total initial abundance $\Omega_{\mathrm{tot}}(t_{\mathrm{prod}}) \equiv \sum_n \Omega_n(t_{\mathrm{prod}})$ of the DDM ensemble at $t=t_{\mathrm{LS}}$ accord with the dark-matter abundance $\Omega_{\mathrm{DM}}(t_{\mathrm{LS}})$ derived from Planck data [28].

III. COSMIC EXPANSION IN THE PRESENCE OF DECAYING ENSEMBLES

Observational data [28] indicate that at large scales our universe is extremely homogeneous, isotropic, and spatially flat. Such a universe is described by a Friedmann-Robertson-Walker (FRW) metric with vanishing spatial curvature. The expansion rate of the universe in an FRW cosmology may be quantified in terms of the Hubble parameter $H = \dot{a}/a$, where a is the scale factor. In such a universe, the luminosity distance $d_L(z)$ of an astrophysical source, expressed as a function of its cosmological redshift $z \equiv (1 - a)/a$, is

$$d_L(z) = \frac{c(1+z)}{H_{\text{now}}} \int_0^z \mathcal{F}^{-1/2}(z') dz', \tag{3.1}$$

where H_{now} is the present-day value of the Hubble parameter and where the quantity

$$\mathcal{F}(z') \equiv \frac{1}{\rho_{\text{crit}}(0)} \sum_{i} \rho_{i}(z')$$
 (3.2)

represents the sum over the energy densities of all relevant cosmological components (photons, baryons, dark matter, etc.), normalized to the value of the critical energy density $\rho_{\rm crit}(0)$ at redshift z=0—i.e., at present time. More specifically, for the toy DDM model defined in Sec. II, we have

$$\mathcal{F}(z) = \frac{1}{\rho_{\text{crit}}(0)} [\rho_{\text{tot}}(z) + \rho_{\psi}(z) + \rho_{b}(z) + \rho_{\gamma}(z) + \rho_{\nu}(z) + \rho_{\Lambda}(z)]$$

$$(3.3)$$

where $\rho_{\text{tot}}(z)$, $\rho_{\psi}(z)$, $\rho_{b}(z)$, $\rho_{\gamma}(z)$, $\rho_{\nu}(z)$, and $\rho_{\Lambda}(z)$ respectively denote the energy densities of the DDM ensemble as a whole, the dark-radiation field ψ , baryons, photons, neutrinos, and dark energy. Thus, in order to determine

the functional relationship between the redshifts and luminosity distances of astrophysical objects for any given choice of parameters within this model, we must assess how each of these energy densities evolves as a function of z.

In general, the energy density of a cosmological component with equation-of-state parameter $w_i(z)$ scales with z according to the relation

$$\rho_i(z) = \rho_i(0)(1+z)^{3[1+w_i(z)]},\tag{3.4}$$

where $\rho_i(0)$ denotes the energy density of that component at present time. For those cosmological components for which $w_i(z)$ is effectively constant since the time of last scattering, $\rho_i(z)$ is trivial to obtain. For example, since $w_b \approx 0$ and $w_\gamma = 1/3$, we have $\rho_b(z) = \rho_b(0)(1+z)^3$ and $\rho_\gamma(z) = \rho_\gamma(0)(1+z)^4$. Likewise, under the assumption that the dark energy behaves like a cosmological constant—i.e., that $w_\Lambda \approx -1$ at all times subsequent to $t_{\rm LS}$ —we have $\rho_\Lambda(z) \approx \rho_\Lambda(0)$ for all z. The present-day energy densities of these cosmological components can be inferred from Planck data [28]. In particular, we find that $\rho_b(0) \approx 2.32 \times 10^{-7}$ GeV cm⁻³ and $\rho_\Lambda(0) \approx 3.24 \times 10^{-6}$ GeV cm⁻³, while the energy density of photons at z=0 is given by

$$\rho_{\gamma}(0) = \frac{4\sigma}{c} T_{\gamma}^{4}(0), \tag{3.5}$$

where $\sigma \approx 0.0354~{\rm GeV~cm^{-2}~s^{-1}~K^{-4}}$ is the Stefan-Boltzmann constant, where c is the speed of light, and where $T_{\gamma}(0) \approx 2.73~{\rm K}$ is the present-day CMB-photon temperature.

The evolution of $\rho_{\nu}(z)$ with z is slightly more complicated due to the presence of small but nonzero masses m_{ν_i} for at least two of the three neutrino mass eigenstates. At early times, all neutrinos species are highly relativistic. At such times, $w_{\nu}(z) \approx 1/3$ and $\rho_{\nu}(z)$ scales with redshift as $\rho_{\nu} \propto (1+z)^4$. Thus, at such times, $\rho_{\nu}(z)$ is proportional to $\rho_{\gamma}(z)$. However, as t increases and the temperature T_{ν} in the neutrino sector drops, $\rho_{\nu}(z)$ eventually begins to deviate significantly from this simple scaling behavior. Indeed, under the assumption that $m_{\nu_i} > 0$ for all three neutrino species, one would expect that $\rho_{\nu} \propto (1+z)^3$ at sufficiently late times. In order to interpolate between the early-time and late-time behavior of $\rho_{\nu}(z)$, it is traditional to introduce a scaling function f(z) such that

$$\rho_{\nu}(z) = \frac{7}{8} \left(\frac{4}{11}\right)^{4/3} N_{\text{eff}} \rho_{\gamma}(z) f(z), \tag{3.6}$$

where $N_{\rm eff} \approx 3.042$ [29] is the effective number of neutrino species. The functional form of f(z) turns out to be well approximated by [30]

$$f(z) \approx \left[1 + \left(\frac{A}{1+z}\right)^p\right]^{1/p},$$
 (3.7)

where $p \approx 1.83$ and where the dimensionless constant A is given by

$$A \approx (1.87 \times 10^5 \text{ eV}^{-1}) \left[\frac{180\zeta(3)}{7\pi^4} \right] \sum_{i=1}^3 m_{\nu_i}.$$
 (3.8)

While the individual neutrino masses m_{ν_i} are not currently known, the sum appearing in Eq. (3.8) is bounded from above by cosmological considerations and from below by neutrino-oscillation data. Bounds in the literature differ slightly depending on the particulars of the analysis method and on whether a normal or inverted neutrino-mass hierarchy is assumed. However, as discussed in Ref. [31] and references therein, this sum is constrained to lie within the rough range

$$0.06 \text{ eV} \lesssim \sum_{i=1}^{3} m_{\nu_i} \lesssim 0.15 \text{ eV}$$
 (3.9)

within the context of a Λ CDM cosmology. For concreteness, we shall adopt $\sum_{i=1}^{3} m_{\nu_i} = 0.1$ eV as our benchmark in what follows.

Finally, we consider the energy densities $\rho_n(z)$ and $\rho_{\psi}(z)$ of the individual ensemble constituents χ_n and the dark-radiation field ψ . These energy densities evolve according system of Boltzmann equations given by

$$\frac{d\rho_n}{dt} + 3H\rho_n = -\Gamma_n \rho_n$$

$$\frac{d\rho_{\psi}}{dt} + 4H\rho_{\psi} = \sum_{n=0}^{N-1} \Gamma_n \rho_n,$$
(3.10)

where collision terms associated with inverse-decay processes of the form $\psi\bar{\psi}\to\chi_n$ have been omitted, as their effect on the ρ_n and on ρ_ψ is negligible. The evolution equation for $\rho_n(t)$ may also be expressed in the equivalent form

$$\frac{d}{dt}(a^3\rho_n) = -\Gamma_n(a^3\rho_n),\tag{3.11}$$

which may be integrated directly in order to obtain an expression for ρ_n as a function of time, or equivalently as a function of the scale factor a. In particular, the expression for $\rho_n(a)$ is found to be

$$\rho_n(a) = \rho_n(a_{LS}) \left(\frac{a_{LS}}{a}\right)^3 e^{-\Gamma_n[t(a)-t_{LS}]},$$
(3.12)

where a_{LS} is the scale factor at last scattering and where t(a) is the time in the background frame expressed as a function of a.

In order to solve the Boltzmann equation for ρ_{ψ} in Eq. (3.10), we begin by changing variables from t to a, yielding

$$\frac{d\rho_{\psi}}{da} = -\frac{4\rho_{\psi}}{a} + \frac{1}{aH} \sum_{n=0}^{N-1} \Gamma_n \rho_n(a). \tag{3.13}$$

Substituting for $\rho_n(a)$ using Eq. (3.12), we have

$$\frac{d\rho_{\psi}}{da} = -\frac{4\rho_{\psi}}{a} + \frac{a_{LS}^{3}\rho_{crit}(a_{LS})\mathcal{F}^{-1/2}(a)}{a^{4}H_{now}} \times \sum_{n=0}^{N-1} \Gamma_{n}\Omega_{n}(t_{LS})e^{-\Gamma_{n}[t(a)-t_{LS}]},$$
(3.14)

where $\mathcal{F}(a)$ is given by Eq. (3.3). We emphasize that not only does the right side of Eq. (3.14) explicitly involve t(a), but it also implicitly involves both t(a) and $\rho_{\psi}(a)$ through $\mathcal{F}(a)$. The form of t(a) in our DDM scenario may be inferred from the relation

$$\frac{dt}{da} = \frac{1}{Ha} = \frac{\mathcal{F}^{-1/2}(a)}{aH_{\text{now}}},$$
(3.15)

the right side of which likewise involves both t(a) and $\rho_{\psi}(a)$ through $\mathcal{F}(a)$. Equations (3.15) and (3.15) may therefore be solved together numerically as a coupled system in order to yield expressions for $\rho_{\psi}(a)$ and t(a) as functions of a, or equivalently as functions of the redshift z. Once these expressions are known, they may be substituted into Eq. (3.1) in order to obtain a functional form for $d_L(z)$.

IV. IMPLEMENTING SUPERNOVA CONSTRAINTS ON DECAYS WITHIN THE DARK SECTOR

A constraint on the functional form of $d_L(z)$ within the recent cosmological past—i.e., at redshifts $0 < z \lesssim 5$ —can be derived from observations of the redshifts and luminosity distances of Type Ia supernovae. The luminosity distance d_L of an astrophysical source can be inferred from its distance modulus μ , which represents the difference between its apparent and absolute magnitude. In particular, the relationship between these two quantities is given by

$$\mu = 5\log_{10}\left(\frac{d_L}{\text{Mpc}}\right) + 25. \tag{4.1}$$

In this analysis, we derive our constraints on $d_L(z)$ from the combined Pantheon sample [32], which contains magnitude and redshift information for $N_{\rm SN}=1048$ spectroscopically confirmed Type Ia supernovae with high-quality light curves.

In order to compare the theoretical relationship between $d_L(z)$ and z obtained for a given choice of our DDM model parameters to the results obtained for the Pantheon data, we proceed as follows. We evaluate the goodness-of-fit statistic

$$\chi^2 = \sum_{j=1}^{N_{\rm SN}} \frac{[\mu_j^{\rm obs} - \mu(z_j)]^2}{(\Delta \mu_j^{\rm obs})^2},\tag{4.2}$$

where the index $j=1,2,\ldots,N_{\rm SN}$ labels the supernovae in the data set, where μ_i^{obs} represents the observed value of the distance modulus for the jth supernova in that set, where $\Delta\mu_j^{
m obs}$ is the uncertainty in $\mu_j^{
m obs}$, and where $\mu(z_j)$ is the predicted value of the distance modulus obtained for the measured redshift z_i of that same supernova within the context of a particular cosmological model. In order to assess how the supernovae in the Pantheon sample constrain the parameter space of our toy DDM model, we proceed as follows. We first obtain a p-value by comparing the value of χ^2 obtained for any particular choice of model parameters to a chi-square distribution with $N_{\text{dof}} = N_{\text{SN}} - 6 = 1042$ degrees of freedom. We then determine the equivalent statistical significance to which this p-value would correspond for a Gaussian distribution. We consider regions of parameter space for which this Gaussian-equivalent statistical significance exceeds 3σ to be excluded.

In surveying the parameter space of our model, two issues arise which require further comment. First, when comparing the $\mu(z_i)$ in the context of any particular model to the corresponding measured values μ_i^{obs} , we must account for systematic uncertainties in the overall normalization of the theoretical $\mu(z)$ curve relative to this set of measured values. Indeed, this relative normalization depends both on the value of $H_{\rm now}$ and on the absolute magnitude of the reference population of Type Ia supernovae against which the μ_i^{obs} are calibrated [33], both of which involve non-negligible uncertainties. It is not our aim in this paper to perform an analysis of these uncertainties or to assess the degree of tension which exists between observational data and the predictions of the standard cosmology, but rather to constrain deviations from the standard cosmology which result from replacing the stable dark-matter candidate with a DDM ensemble on the basis of Type Ia supernova data alone. Thus, in our analysis, we shall adopt a conservative approach to constraining these deviations in which we adjust the μ_i^{obs} by an overall additive constant chosen such that the goodness-of-fit statistic χ^2 defined in Eq. (4.2) is minimized for a stable dark-matter candidate in the Λ CDM cosmology. Possible alternative approaches in which additional cosmological parameters are also allowed to vary will be discussed in Sec. VI. We note that as a result of our taking this conservative approach, the bounds we obtain on the lifetime of a single unstable particle species which decays to two massless daughter particles are slightly weaker than those obtained in Ref. [26].

The second issue that we must address concerns our initial conditions for the ensemble. Planck data place stringent constraints on the abundances of both dark matter and dark radiation at $t=t_{\rm LS}$. Deviations in the present-day dark matter abundance $\Omega_{\rm DM}(t_{\rm now})h^2\approx 0.120$ inferred from CMB data are constrained at the percent level [28], implying a similar bound on deviations from the dark-matter abundance at $t=t_{\rm LS}$. The corresponding constraint on the abundance of dark radiation is typically phrased as a bound on the net additional contribution $\Delta N_{\rm eff}$ to the effective number of neutrino species $N_{\rm eff}$ from particles other than SM neutrinos. The current bound $\Delta N_{\rm eff}\lesssim 0.28$ [28] implies a constraint

$$\frac{\Omega_{\psi}(t_{\rm LS})}{\Omega_{\rm v}(t_{\rm LS})} \lesssim 0.15\tag{4.3}$$

on the abundance of the dark-radiation field ψ within our DDM model at the 95% confidence level, where $\Omega_{\gamma}(t_{\rm LS})$ denotes the abundance of photons at $t=t_{\rm LS}$. Taken together, these constraints imply that the cosmology of our DDM model should not differ significantly from that of a Λ CDM universe at $t \lesssim t_{\rm LS}$.

The early decays of the χ_n —and especially those with lifetimes in the regime $\tau_n \lesssim t_{\rm LS}$ —can lead to a significant reduction in the total dark-matter abundance at last scattering and generate a significant abundance for dark radiation by $t = t_{LS}$. We must therefore ensure that the collective effect of these early decays on the cosmology of our DDM scenario at times $t \lesssim t_{LS}$ is negligible. In doing so, we proceed as follows. We begin by defining the extrapolated abundance $\tilde{\Omega}_n(t)$ of χ_n at time t, which represents the abundance that this ensemble constituent would have had at time t if it were absolutely stable. We fix the initial value $\Omega_0(t_{\rm prod})$ by demanding that the total extrapolated abundance $\Omega_{\text{tot}}(t) \equiv \Omega_n(t)$ of the ensemble is equal to the central value for $\Omega_{\rm DM}(t_{\rm LS})$ inferred from Planck data. We then calculate the actual abundances $\Omega_{\mathrm{tot}}(t_{\mathrm{LS}})$ and $\Omega_{\psi}(t_{\mathrm{LS}})$ accounting for the effect of χ_n decay. In doing so, we approximate the universe as radiation-dominated, with $a \propto t^{1/2}$, prior to the time $t_{\rm MRE}$ of matter-radiation equality, and as matter-dominated, with $a \propto t^{2/3}$, for $t_{\text{MRE}} < t < t_{\text{LS}}$. For any given choice of model parameters, we define a small cutoff parameter 무 and then impose a constraint

$$1 - \frac{\Omega_{\text{tot}}(t_{\text{LS}})}{\widetilde{\Omega}_{\text{tot}}(t_{\text{LS}})} \le \mp \tag{4.4}$$

¹We have chosen the Korean word $\stackrel{\square}{\vdash}$, pronounced "mu" and meaning "void" or "empty," as our notation for this parameter, since its purpose is to ensure that the universe is essentially devoid or empty of dark radiation at times $t \lesssim t_{LS}$.

on the portion of the overall dark-matter abundance that has be depleted by decays prior to last scattering. Any ensemble which does not satisfy this criterion is considered to be inconsistent with our initial conditions and therefore excluded. Given the aforementioned constraint on the dark-matter abundance, we take $\frac{1}{1}=0.01$. We note that for this value of $\frac{11}{1}$, the constraint in Eq. (4.4) is always more stringent than the corresponding constraint on $\Omega_{\psi}(t_{\rm LS})$ from Eq. (4.3).

V. RESULTS

We begin the discussion of our results by examining how the goodness of fit between the theoretical distance-modulus function $\mu(z)$ and the Pantheon data varies across the parameter space of our DDM model. In Fig. 1, we display curves showing the value of $\chi^2/N_{\rm dof}$ as a function of $\tau_0 \equiv$ Γ_0^{-1} for different choices of the model parameters N (top panel) and γ (bottom panel) which essentially control the distribution of $\Omega_{\rm tot}(t_{\rm LS})$ across the ensemble. The results shown in the top panel correspond to the choices $\gamma = -2$, $\Delta m/m_0 = 1$, and $\xi = 3$; the results shown in the bottom panel correspond to the choices N = 10 and the same values of $\Delta m/m_0$ and ξ . In each panel, for reference, we have also included a (dashed black) curve showing $\chi^2/N_{\rm dof}$ for a single dark-matter particle species with lifetime τ_0 . The lower dashed horizontal line in each panel indicates the value of $\chi^2/N_{\rm dof}$ obtained for a stable dark-matter particle in the standard cosmology, while the other dashed horizontal lines indicate the values of $\chi^2/N_{\rm dof}$ for which the corresponding p-values would be associated with the statistical significances 3σ and 5σ for a Gaussian distribution.

The results shown in the top panel of Fig. 1 illustrate the impact on $\chi^2/N_{\rm dof}$ of introducing additional, unstable states into the ensemble. The results shown indicate that the value of $\chi^2/N_{\rm dof}$ is quite sensitive to the value of N in the regime in which N is small, but becomes less sensitive as N increases. By contrast, the results shown in the bottom panel illustrate that $\chi^2/N_{\rm dof}$ becomes increasingly sensitive to the value of γ as γ increases.

In Fig. 2, we display the constraints on the parameter space of our DDM model from the Pantheon data sample. The contour plot in each panel of the figure shows the 3σ lower bound τ_0^{\min} on τ_0 within the (ξ, γ) -plane for a particular choice of N and $\Delta m/m_0$. The results displayed in the different columns of the figure from left to right respectively correspond to the parameter choices $N = \{2, 10, 10^5\}$. Likewise, the results displayed in the different rows of the figure from top to bottom respectively correspond to the parameter choices $\Delta m/m_0 = \{0.1, 1, 10\}$.

Interpreting the results shown in Fig. 2, we first note that within each individual panel of the figure, $\tau_0^{\rm min}$ generically increases as both ξ and γ are increased. This is to be expected: increasing γ redistributes a larger fraction of $\Omega_{\rm tot}(t_{\rm LS})$ to the heavier, more unstable modes in the

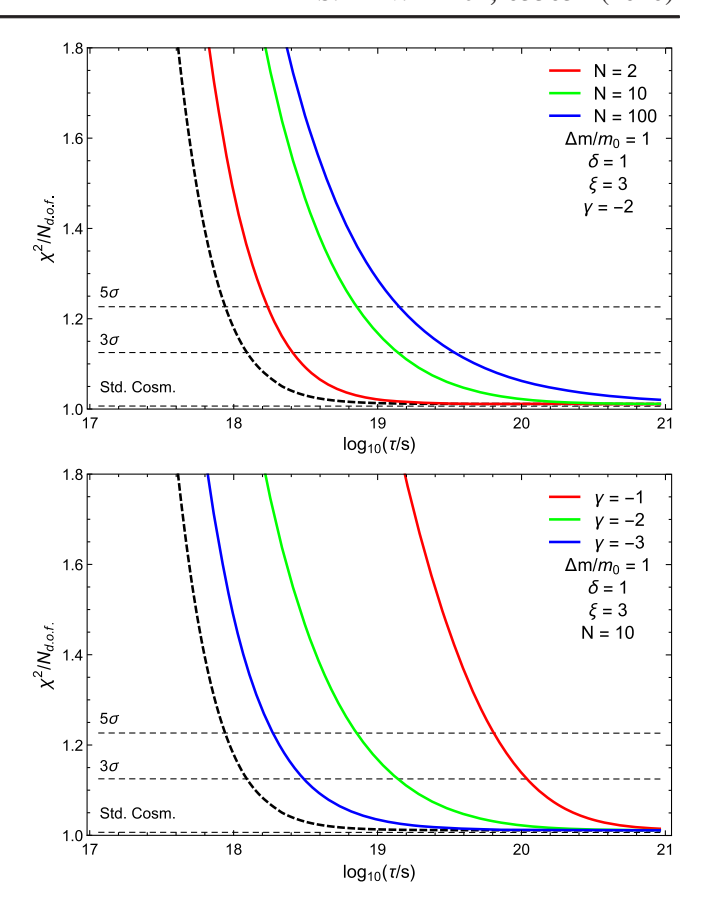


FIG. 1. The goodness of fit $\chi^2/N_{\rm dof}$ between the distancemodulus function $\mu(z)$ obtained for a particular set of DDM model parameters and the data in the Pantheon sample, plotted as functions of the lifetime τ_0 of the lightest particle in the DDM ensemble. The curves shown in the top panel correspond to different values of N for fixed $\gamma = -2$, $\Delta m/m_0 = 1$, and $\xi = 3$. The curves shown in the bottom panel correspond to different values of γ for fixed N=10 and the same values of $\Delta m/m_0$ and ξ . In each panel, the corresponding curve for a single dark-matter particle species with lifetime τ_0 is indicated by the black dashed curve. For reference, within each panel we have also included dashed lines showing the values of $\chi^2/N_{\rm dof}$ which correspond to a discrepancy between the theoretical $\mu(z)$ function and the Pantheon data at the 3σ and 5σ significance levels, along with another dashed line indicating the value of $\chi^2/N_{\rm dof}$ obtained for a stable dark-matter candidate in the standard cosmology.

ensemble, while increasing ξ decreases the lifetimes of these heavier modes. Likewise, comparing the results across different panels of the figure, we see that τ_0^{\min} generically increases as we move from left to right across the panels within any given row of the figure—i.e., as we increase N while holding $\Delta m/m_0$ fixed. Indeed, this behavior accords with the results shown in the top panel of Fig. 1.

However, the way in which τ_0^{max} changes as we move from top to bottom along the panels within a given column of the figure—i.e., as we increase $\Delta m/m_0$ while holding N fixed—is far less straightforward and depends nontrivially on the value of N. When $\Delta m/m_0$ is taken to be sufficiently

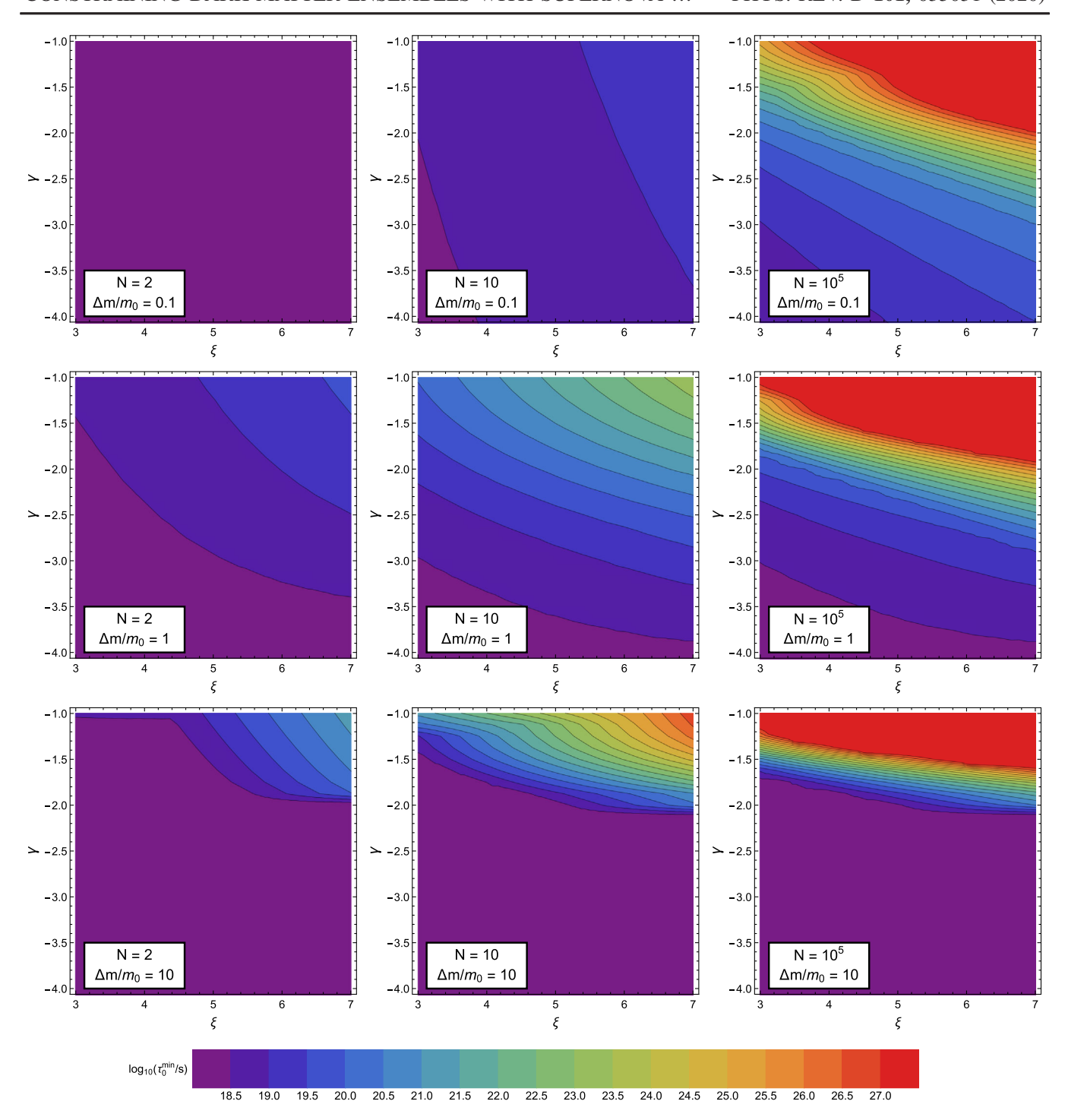


FIG. 2. Constraints on the parameter space of our DDM model from supernova data. In each panel, the contour plot shows the 3σ lower bound τ_0^{\min} on the lifetime of the lightest particle in the ensemble for a particular choice of N and $\Delta m/m_0$. The results displayed in the different columns of the figure from left to right respectively correspond to the parameter choices choices $N = \{2, 10, 10^5\}$. Likewise, the results displayed in the different rows of the figure from top to bottom respectively correspond to the parameter choices $\Delta m/m_0 = \{0.1, 1, 10\}$. We see that our constraints are generally most severe for ensembles with intermediate values of $\Delta m/m_0 \sim \mathcal{O}(1-10)$ and large values of ξ and γ .

small for any finite value of N, the lifetimes of all of the χ_n with n > 0 are comparable to τ_0 . Thus, in this regime, the ensemble effectively behaves like a single unstable particle with lifetime τ_0 in terms of its effect on the expansion

history of the universe. Moreover, in this regime, $\tau_0^{\rm max}$ is fairly insensitive to the values of γ and ξ . The results shown in the top left panel of the figure, which correspond to the parameter choices N=2 and $\Delta m/m_0=0.1$, are

representative of this regime. The larger N is, however, the greater the range of masses present within the ensemble and the smaller $\Delta m/m_0$ must therefore be in order for the ensemble to remain in this regime. Indeed, even for N=10, we see that $\Delta m/m_0$ is sufficiently large that $\tau_0^{\rm max}$ exhibits a nontrivial dependence on ξ and γ .

On the other hand, for intermediate values of $\Delta m/m_0 \sim \mathcal{O}(1\text{--}10)$ we observe that the results for τ_0^{max} can differ considerably from the corresponding constraints on a single decaying particle. Indeed, for such values of $\Delta m/m_0$, the χ_n with n>0 not only collectively represent a non-negligible fraction of $\Omega_{\text{tot}}(t_{\text{LS}})$ within the region shown in each panel, but also exhibit a broad range of lifetimes. Thus, it is for DDM ensembles with $\Delta m/m_0 \sim \mathcal{O}(1\text{--}10)$ that supernova data are generally the most constraining.

It is also worth noting that it is within this intermediate- $\Delta m/m_0$ regime—and especially when N is small—that the constraint in Eq. (4.4) has a significant impact on the value of τ_0^{max} . In the panel of Fig. 2 corresponding to N=2 and $\Delta m/m_0 = 10$, for example, this constraint plays a crucial role in establishing the lifetime bound obtained within the region of the (ξ, γ) -plane wherein ξ is large and $\gamma \lesssim -2$. This can be understood as follows. In the regime in which $\Delta m/m_0 \gtrsim 1$, an extreme value of ξ is not required in order to achieve a significant difference between the lifetimes of the lightest two constituents in the DDM ensemble. Indeed, for any fixed value for τ_0 , the lifetime τ_1 of χ_1 decreases as ξ increases and eventually becomes comparable to $t_{\rm LS}$. This implies that a significant fraction of the abundance $\tilde{\Omega}_1(t_{LS})$ which this ensemble constituent would have had at last scattering had it been stable is instead converted to dark radiation prior to t_{LS} . For $\gamma \geq -2$, this $\tilde{\Omega}_1(t_{LS})$ represents a sufficiently large fraction of $\tilde{\Omega}_{tot}(t_{LS})$ that a sizable value of τ_0 is required in order not to violate the constraint in Eq. (4.4). This constraint also imposes a similar lower bound on τ_0 in the other panels of Fig. 2 for which $\Delta m/m_0 = 10$, but this bound is superseded by the 3σ lower bound on τ_0 from the Pantheon data throughout most of the same region of the (ξ, γ) -plane for both N = 10 and $N = 10^5$.

The au_0^{\max} contours obtained for even larger values of $\Delta m/m_0$ follow the general trends exhibited in Fig. 2. Indeed, when $\Delta m/m_0\gg 1$, the vast majority of $\Omega_{\rm tot}(t_{\rm LS})$ is carried by χ_0 unless the value of γ is quite large. As a result, the bound on τ_0 typically becomes weaker with increasing $\Delta m/m_0$ within this regime. Thus, if one were to plot contours of τ_0^{\max} for $\Delta m/m_0\gg 1$ similar to those shown in Fig. 2, one would find that the value of τ_0^{\max} would not significantly differ from the lower bound on the lifetime of a single unstable particle which decays to dark radiation throughout most of the same region of the (ξ,γ) -plane, regardless of the value of N.

Given the results in Fig. 2, it is likewise straightforward to infer the behavior of the corresponding τ_0^{\max} contours for even larger values of N. As illustrated in Fig. 1, τ_0^{\max} becomes largely insensitive to N in the regime in which N

is large. Indeed, provided that $\gamma < -1$ and that the sum over $\Omega_n(t_{\mathrm{prod}})$ converges in the $N \to \infty$ limit, one finds that τ_0^{max} approaches a finite asymptotic value this limit. Thus, for any particular choice of the remaining model parameters, the value of τ_0^{max} obtained for sufficiently large, finite N is effectively equal to this asymptotic value. Throughout most the region of the (ξ,γ) -plane shown in the panels of Fig. 2, the number $N=10^5$ turns out to be sufficiently large that the value of τ_0^{max} obtained for this choice of N lies within this asymptotic regime. Indeed, only when γ approaches the value $\gamma=-1$ at which the sum over $\Omega_n(t_{\mathrm{prod}})$ formally diverges do the results for τ_0^{max} begin to deviate significantly from those obtained in the $N\to\infty$ limit.

The results shown in Fig. 2 demonstrate that meaningful bounds on the parameter space of DDM ensembles can be derived from constraints on the expansion history of the universe—and in particular on the relationship the between redshifts and luminosity distances of Type Ia supernovae—even in situations in which the decays of the ensemble constituents decay entirely to other light states within a hidden sector. These bounds turn out to be the most constraining for ensembles with intermediate values of $\Delta m/m_0 \sim \mathcal{O}(1-10)$ and large values of ξ and γ .

VI. CONCLUSIONS

In this paper, we have considered the constraints on DDM ensembles whose constituent particles decay primarily to other, lighter particles within the dark sector by analyzing the constraints on such ensembles which arise from the effects of these decays on the expansion history of the universe. In particular, we have derived constraints on the parameter space of such ensembles from the relationship between the observed redshifts and luminosity distances of Type Ia supernovae within the Pantheon data sample.

Several comments are in order. First, we note that a variety of other considerations can also be used to constrain the decays of dark-sector particles to other states within the dark sector. For example, baryon acoustic oscillations and the properties of the CMB both provide information about the expansion history of the universe. These considerations have been used to constrain dark-matter decays within single-component dark-matter scenarios [27], and it would be interesting to examine the extent to which these complementary probes of the expansion history at different redshifts constrain the parameter space of DDM ensembles as well. In addition, decays within the dark sector can also give rise to characteristic features within the matter power spectrum which can yield information about the structure of the decaying ensemble [34].

In addition, in this paper we have focused on ensembles in which each constituent χ_n decays exclusively to dark radiation. As discussed in Sec. II, the corresponding constraints on ensembles in which the χ_n can also decay into final states involving other, lighter ensemble constituents are

always less stringent, given that decays directly to dark radiation represent the most efficient conversion possible of mass energy into kinetic energy. It would nevertheless be interesting to investigate the supernova constraints on ensembles in which intra-ensemble decays play a significant role in the decay phenomenology of the χ_n .

Finally, as discussed in Sec. IV, in this paper we have focused on modifications of the standard cosmology in which the stable dark-matter candidate is replaced with a DDM ensemble, but in which no further modifications are made. Moreover, we have assumed that the values of the relevant nuisance parameters are such that the $d_L(z)$ function obtained for the standard cosmology provides a good fit to the Pantheon data. These include several nuisance parameters involved in determining the $\mu_i^{\rm obs}$ for the supernovae in the Pantheon sample. While this is common practice [26,35], we note that the assessment of the statistical likelihood for any cosmological model can be improved by simultaneously fitting the values of these nuisance parameters along with with the values of the parameters which characterize that model [36,37]. While the complexity of our DDM model renders such an analysis impractical for a survey of the sort we have undertaken in this paper, a study along these lines would be an interesting avenue for future research.

Along the same lines, while this minimal approach is fruitful for constraining deviations from the standard cosmology within the DDM framework, there are compelling reasons why it would be interesting to consider a more general study in which other cosmological parameters are allowed to vary. For example, a statistically significant tension currently exists between the value of H_{now} obtained from local probes of the cosmic expansion rate (including not only Type Ia supernova data [38–41], but also lensing time-delay experiments [42,43]) and the value inferred from CMB data in the context of a Λ CDM cosmology [44–47]. Dark-matter decays between t_{LS} and t_{now} have been posited as one possible [48–53] way of alleviating these tensions.

While it has not been our aim in this paper to address the Hubble tension, it likely that DDM scenarios of the sort can serve to alleviate this tension. In order to understand why this occurs, we begin by noting that in addition to constraining the energy density of dark matter at last scattering, CMB data also tightly constrain the angular horizon size θ_s , which in a flat universe may be written as

$$\theta_s = \frac{(1+z_{\rm LS})r_{\rm LS}}{d_L(z_{\rm LS})},$$
(6.1)

where $r_{\rm LS}$ is the sound horizon and where $d_L(z_{\rm LS})$ is the luminosity distance of the last-scattering surface. Since the sound horizon is determined by the state of the universe prior to last scattering, the value of $r_{\rm LS}$ obtained in our DDM scenario does not differ appreciably from that

obtained in the standard cosmology for the same choice of cosmological parameters. By contrast, $d_L(z_{\rm LS})$ depends on the state of the universe at all redshifts $0 < z < z_{\rm LS}$. Thus, its value for a given choice of DDM model parameters in general differs—potentially significantly—from that obtained in the standard cosmology.

In our DDM scenario, decays of the χ_n between t_{LS} and t_{now} transfer energy density from dark matter to dark radiation. Since ρ_{ψ} decreases more rapidly as a result of cosmic expansion than does ρ_{ν} , the expansion rate of the universe is lower in our DDM scenario at low redshifts than it would have been in a ACDM scenario with the same value $H(z_{LS})$ of the Hubble parameter at last scattering. However, a consistently lower value of H(z) at late times results in a larger value for $d_L(z_{LS})$. This in turn results in a smaller value for θ_s . Thus, in order to obtain a value of θ_s which accords with Planck data in our DDM scenario, we need to compensate for this decrease by increasing the dark-energy density ρ_{Λ} , which in turn increases $H(z_{LS})$. The larger ρ_{Λ} implies that dark energy will begin to dominate the universe at a slightly earlier time than it otherwise would in the standard cosmology, and consequently yields a larger value of H_{now} . In this sense, our DDM scenario modifies the cosmic expansion rate in the right direction for addressing the Hubble tension.

We note that this basic mechanism through which DDM can alleviate the Hubble tension is the same as that which underlies other scenarios for alleviating this tension through decaying dark matter. The primary difference, however, is that the DDM framework allows the conversion of dark matter to dark radiation to occur more smoothly over a longer timescale. Of course, more quantitative statements concerning the degree to which a DDM ensemble can alleviate the Hubble tension would require a more detailed study including an analysis of how the decays of the χ_n would collectively impact the properties of the CMB, the matter power spectrum, and other cosmological observables. We leave such a study for future work.

ACKNOWLEDGMENTS

We are happy to thank S. Koushiappas for discussions. A. D. also wishes to thank the EXCEL Scholars Program for Undergraduate Research at Lafayette College, which helped to facilitate this research. The research activities of A. D. and B. T. are supported in part by the National Science Foundation under Grant PHY-1720430. The research activities of K. R. D. are supported in part by the Department of Energy under Grant DE-FG02-13ER41976 (DE-SC0009913) and by the National Science Foundation through its employee IR/D program. The opinions and conclusions expressed herein are those of the authors, and do not represent any funding agencies.

- [1] K. R. Dienes and B. Thomas, Phys. Rev. D **85**, 083523 (2012).
- [2] K. R. Dienes and B. Thomas, Phys. Rev. D **85**, 083524 (2012).
- [3] K. R. Dienes, S. Su, and B. Thomas, Phys. Rev. D 86, 054008 (2012).
- [4] K. R. Dienes, S. Su, and B. Thomas, Phys. Rev. D **91**, 054002 (2015).
- [5] D. Curtin et al., Rep. Prog. Phys. 82, 116201 (2019).
- [6] D. Curtin, K. R. Dienes, and B. Thomas, Phys. Rev. D 98, 115005 (2018).
- [7] K. R. Dienes, J. Kumar, and B. Thomas, Phys. Rev. D 86, 055016 (2012).
- [8] K. R. Dienes, J. Kumar, and B. Thomas, Phys. Rev. D 88, 103509 (2013).
- [9] K. K. Boddy, K. R. Dienes, D. Kim, J. Kumar, J. C. Park, and B. Thomas, Phys. Rev. D 95, 055024 (2017).
- [10] K. K. Boddy, K. R. Dienes, D. Kim, J. Kumar, J. C. Park, and B. Thomas, Phys. Rev. D 94, 095027 (2016).
- [11] M. Ackermann *et al.* (Fermi-LAT Collaboration), Astrophys. J. **799**, 86 (2015).
- [12] T. Cohen, K. Murase, N. L. Rodd, B. R. Safdi, and Y. Soreq, Phys. Rev. Lett. 119, 021102 (2017).
- [13] M. Cirelli, E. Moulin, P. Panci, P. D. Serpico, and A. Viana, Phys. Rev. D 86, 083506 (2012).
- [14] W. Liu, X. J. Bi, S. J. Lin, and P. F. Yin, Chin. Phys. C 41, 045104 (2017).
- [15] C. Blanco and D. Hooper, J. Cosmol. Astropart. Phys. 03 (2019) 019.
- [16] R. Essig, E. Kuflik, S. D. McDermott, T. Volansky, and K. M. Zurek, J. High Energy Phys. 11 (2013) 193.
- [17] T. R. Slatyer and C. L. Wu, Phys. Rev. D 95, 023010 (2017).
- [18] M. Aguilar *et al.* (AMS Collaboration), Phys. Rev. Lett. 110, 141102 (2013).
- [19] M. Aguilar *et al.* (AMS Collaboration), Phys. Rev. Lett. 122, 041102 (2019).
- [20] A. Ibarra, A. S. Lamperstorfer, and J. Silk, Phys. Rev. D 89, 063539 (2014).
- [21] Y. Gong and X. Chen, Phys. Rev. D 77, 103511 (2008).
- [22] V. Poulin, P.D. Serpico, and J. Lesgourgues, J. Cosmol. Astropart. Phys. 08 (2016) 036.
- [23] K. R. Dienes and B. Thomas, Phys. Rev. D 86, 055013 (2012).
- [24] K. R. Dienes, F. Huang, S. Su, and B. Thomas, Phys. Rev. D 95, 043526 (2017).
- [25] K. R. Dienes, J. Fennick, J. Kumar, and B. Thomas, Phys. Rev. D 97, 063522 (2018).
- [26] G. Blackadder and S. M. Koushiappas, Phys. Rev. D 90, 103527 (2014).

- [27] G. Blackadder and S. M. Koushiappas, Phys. Rev. D 93, 023510 (2016).
- [28] P. A. R. Ade *et al.* (Planck Collaboration), Astron. Astrophys. **594**, A13 (2016).
- [29] G. Mangano, G. Miele, S. Pastor, and M. Peloso, Phys. Lett. B **534**, 8 (2002).
- [30] E. Komatsu *et al.* (WMAP Collaboration), Astrophys. J. Suppl. Ser. **192**, 18 (2011).
- [31] S. Vagnozzi, S. Dhawan, M. Gerbino, K. Freese, A. Goobar, and O. Mena, Phys. Rev. D **98**, 083501 (2018).
- [32] D. M. Scolnic et al., Astrophys. J. 859, 101 (2018).
- [33] R. Tripp, Astron. Astrophys. 331, 815 (1998), http://aa.springer.de/papers/8331003/2300815.pdf.
- [34] K. R. Dienes, F. Huang, J. Kost, S. Su, and B. Thomas, arXiv:2001.02193.
- [35] F. Melia, Astron. J. 144, 110 (2012).
- [36] J. J. Wei, X. F. Wu, F. Melia, and R. S. Maier, Astron. J. 149, 102 (2015).
- [37] F. Melia, J. J. Wei, R. Maier, and X. Wu, Europhys. Lett. 123, 59002 (2018).
- [38] A. G. Riess et al., Astrophys. J. 826, 56 (2016).
- [39] A. G. Riess et al., Astrophys. J. 861, 126 (2018).
- [40] A. G. Riess, S. Casertano, W. Yuan, L. M. Macri, and D. Scolnic, Astrophys. J. 876, 85 (2019).
- [41] E. Ó. Colgáin, J. Cosmol. Astropart. Phys. 09 (2019) 006.
- [42] V. Bonvin et al., Mon. Not. R. Astron. Soc. 465, 4914 (2017).
- [43] S. Birrer et al., Mon. Not. R. Astron. Soc. 484, 4726 (2019).
- [44] G. Efstathiou, Mon. Not. R. Astron. Soc. 440, 1138 (2014).
- [45] G. E. Addison, Y. Huang, D. J. Watts, C. L. Bennett, M. Halpern, G. Hinshaw, and J. L. Weiland, Astrophys. J. 818, 132 (2016).
- [46] N. Aghanim *et al.* (Planck Collaboration), Astron. Astrophys. 607, A95 (2017).
- [47] K. Aylor, M. Joy, L. Knox, M. Millea, S. Raghunathan, and W. L. K. Wu, Astrophys. J. 874, 4 (2019).
- [48] K. Enqvist, S. Nadathur, T. Sekiguchi, and T. Takahashi, J. Cosmol. Astropart. Phys. 09 (2015) 067.
- [49] L. A. Anchordoqui, V. Barger, H. Goldberg, X. Huang, D. Marfatia, L. H. M. da Silva, and T. J. Weiler, Phys. Rev. D 92, 061301 (2015); 94, 069901(E) (2016).
- [50] J. Buch, P. Ralegankar, and V. Rentala, J. Cosmol. Astropart. Phys. 10 (2017) 028.
- [51] T. Bringmann, F. Kahlhoefer, K. Schmidt-Hoberg, and P. Walia, Phys. Rev. D 98, 023543 (2018).
- [52] K. L. Pandey, T. Karwal, and S. Das, arXiv:1902.10636.
- [53] K. Vattis, S. M. Koushiappas, and A. Loeb, Phys. Rev. D 99, 121302 (2019).